Ferrocenoyl-amino acids: redox response towards di- and trivalent metal ions

Francis E. Appoh, Todd C. Sutherland, Heinz-Bernhard Kraatz *

Department of Chemistry, 110 Science Place, University of Saskatchewan, Sask., Canada S7N 5C9

Abstract

The interaction of six ferrocene-amino acid conjugates (Fc–CO–Gly–OH (**2a**), Fc–CO–Asp–OH (**3a**), Fc–CO–Glu–OH (**4a**), 1,1′-Fc(CO–Gly–OH) (**2b**), 1,1′-Fc(CO–Asp–OH) (**3b**), and 1,1′-Fc(CO–Glu–OH) (**4b**)) with Mg^{2+}, Ca^{2+}, Zn^{2+}, La^{3+}, and Tb^{3+} was investigated in aqueous solutions using cyclic voltammetry (CV) and differential pulse voltammetry (DPV). Addition of metal ions to solutions caused, in some cases, large changes in the half-wave potential, $E_{1/2}$. Our electrochemical results show that the Gly systems, **2a** and **2b**, show a preference for binding Mg^{2+}, whereas the Asp and Glu conjugates prefer binding Ln^{3+}.
© 2004 Elsevier B.V. All rights reserved.

Keywords: Ferrocene; Amino acid; Bioconjugate; Metal binding; Electrochemistry

1. Introduction

In recent years, there has been an interest in the electrochemical detection of ion binding to a ligand which is equipped with a redox active group, such as ferrocene (Fc) or cobaltocene [1–11]. The specificity of the system is dictated by the ligand–ion interactions and detection sensitivity depends on the efficiency of the electronic communication between the ligand–ion complex and the redox group, either through-space or through-bond. Various Fc substituted macrocycles such as cyclams [2], cryptands [1,3], aza-crowns [4], crown ethers [12], and calixarenes [9] have been shown to electrochemically sense the coordination of alkaline-, alkaline earth-, transition-metals and lanthanide ions. Furthermore, peptides are known to show specificity towards metal binding, as was determined by titration experiments using NMR [5–7], potentiometry [11], luminescence measurements [8] FT-IR, CD and UV–vis spectroscopy [10]. Recently, poly-L-aspartate was shown to complex metals like Eu^{3+}, Ce^{3+}, La^{3+}, Cu^{2+}, and Pb^{2+}, and to act as corrosion inhibitors for steel and iron, a property that has been ascribed to the carboxylate side chain of aspartic acid [13,14]. More recently, poly-L-aspartic acid and Gly-Gly-His immobilized films have found use as an electrochemical Cu^{2+} sensor [15,16]. Some metal complexes of Fc amino acid conjugates have been reported in the literature over the years. Ferrocenylimines of the amino acids Gly, Ala, Leu and Val and ferrocenylmethyl amino acid conjugates of Ala and Pro were exploited by Beck and coworkers as ligands for Pd(II) [17] giving a series of mononuclear or binuclear complexes in which N,O-chelation of the ligand was observed. Similarly, metal complexes of bisdimethyl ferrocenoyl derivatives of Gly, Ala, Phe and Tyr were used for their antibacterial properties [18]. In addition, Hirao and co-workers [19] reported a Pd(II) complex of a Fc–peptide–pyridine conjugate.

Aspartate (Asp) and glutamate (Glu) side chains are among the most common amino acid ligands that

---

* Corresponding author. Tel.: +1 306 966 4660; fax: +1 306 966 4730.

E-mail address: kraatz@skyway.usask.ca (H.-B. Kraatz).

coordinate to co-factors in metalloproteins, where they play various roles. The EF-hand proteins, such as calmodulin and Troponin C, are known to contain Asp/Glu side chains which are selective for Ca(II) binding. Furthermore, the Glu residue in calmodulin binds to Ca(II) in a bidentate fashion and is known to lead to a series of reactions whereas the protein is not active when coordinated to Mg(II) thus, demonstrating the selectivity of the proteins [20–22]. The apparent similarities between Ca(II) and lanthanides, particularly with regards to ionic radii, ligand exchange rates, and coordination numbers, have justified its isomorphous replacement in biological macromolecules. For example, it has been shown that Tb(III) is able to displace Ca(II) in the calcuim binding sites of α- and β-crystallins (a protein responsible for opacity in eye lenses) [23]. In addition, it has been reported that La^{3+} increases the activity of phosphodiesterase by competing with Ca^{2+} at low concentrations [24] and it has been shown that La^{3+} improves the capture of light energy of chlorophyll by replacing Mg^{2+} [25]. Zn(II) has also been shown to dislodge Mg(II) from various binding sites of proteins that contain Asp/Glu residues [26,27]. Thus, we asked two simple questions: (a) Is it possible to use electrochemical methods to observe metal binding to ferrocene–peptide conjugates in solution? (b) Do these systems display specificity towards certain metals? To investigate these questions we used ferrocenecarboxylic acid and 1,1′-ferrocenedicarboxylic acid conjugates of the amino acids Gly, Asp and Glu. Asp and Glu are acidic amino acids, which are expected to interact strongly with alkaline earth and lanthanide metal ions. Previously, the Fc group was shown to be sensitive to its environment by efficient electronic coupling through the peptidic backbone and we expect changes in the redox potential upon metal coordination. Since all measurements are to be carried out in water and the amino acids carry ionizable groups, it was important to study the pH dependence of the redox potential. We chose to study the binding of the following metals to the Fc–amino acid conjugates: Mg(II), Ca(II), Zn(II), La(III) and Tb(III) because of their biological relevance described above. This paper presents the results of our study and shows that the Fc–amino acid conjugates show selectivity for different ions.

2. Experimental

2.1. General procedure

The ferrocenoyl amino acids Fc–CO–Gly–OEt (**2a-OEt**) [28–30]. Fc–CO–Gly–OH (**2a**) [28,29], Fc–CO–Asp(OMe)$_2$ (**3a-OMe**), Fc–CO–Asp–OH (**3a**) [31], Fc–CO–Glu(OEt)$_2$ (**4a-OEt**) [32] were all prepared according to the literature procedures, 1,1′-Fc(CO–Gly–OEt)$_2$ (**2b-OEt**) and 1,1′-Fc(CO–Gly–OH)$_2$ (**2b**) were synthesized as reported before [33,34]. Full details of their characterization are given in supplemental material.

2.2. Synthesis of 1,1′-Fc(CO–Asp–OBz)$_2$ (3b-OBz)

To a stirring slurry of 1,1′-Fc(COOH)$_2$ (0.57 g, 1 mM) in CH_2Cl_2 (25 ml), HOBt (0.27 g, 2.1 mM) and EDC (0.42 g, 2.1 mM) were added at 0 °C. H-Asp(OBz)-OBz · Tos (2.33 g, 4.8 mM) was dissolved in 5 ml CH_2Cl_2 and 1 ml Et_3N. The clear solution was transferred into the reaction mixture. The solution was allowed to warm up and stirring was continued overnight. After a standard aqueous work up (saturated $NaHCO_3$ aq., 10% citric acid solution, saturated NaHCO$_3$, followed by distilled water, collection and drying of the organic layer), the crude material was purified by column chromatography (hexane/EtOAc 1:1; $R_f = 0.3$). Yield: 1.30 g, 77%. HR-MS (FAB): calc. for $C_{48}H_{44}N_2O_{10}Fe = 864.2345$, found: 865.1537. FT-IR (cm^{-1}, KBr): 3446 (NH), 1761 (s, C=O ester), 1646 (s, Amide I), 1559 (s, Amide II). UV–vis (CH_3OH, λ_{max} in nm, (ε) in cm^{-1}M^{-1}): 449 (305). ^{1}H NMR (DMSO-d$_6$, δ in ppm): 8.30 (2H, t, $J = 9$ Hz, NH,), 4.80 (2H, s, H^o Cp), 4.78 (2H, s, H^m Cp), 4.29 (4H, s, H^m Cp), 5.14 (4H, m, OCH$_2$ Bz), 5.10 (4H, m, OCH$_2$, Bz), 4.86 (2H, d, CH$^\alpha$-Asp), 3.06, 2.92 (2H, dd, $J = 8$ Hz, CH$_2$ Asp), 7.35 (20H, m, CH Bz). ^{13}C{^{1}H} NMR (δ in ppm, DMSO-d$_6$): 171.6, 170.9, 169.7 (C=O), 136.7 (ipso C–Ph), 129.7, 128.7 (C–Ph), 77.2 (ipso-C^i), 73.1 (C^o), 70.6 (C^m), 67.3, 66.7 (CH$_2$–O ester), 49.8 (C$^\alpha$ of Asp), 36.5 (CH$_2$ Asp).

2.3. Synthesis of 1,1′-Fc(CO–Asp–OH)$_2$ (3b)

1.36 g, (1.58 mM) of **3b-OBz** was added to a Parr hydrogenation chamber and 10% wt palladium/carbon catalyst added. Wet methanol (50 ml) was added and after evacuation, the bomb was pressurized with H$_2$ to 60 psi for 18 h. The progress of the reaction was determined by TLC with 10% CH_3OH/CHCl$_3$. The final product was purified by column chromatography (CH$_3$OH/CHCl$_3$ 1:9, $R_f = 0.4$). Yield: 0.66 g, 83%. HR-MS (FAB) calc. for $C_{20}H_{18}N_2O_{10}Fe = 504.6039$, found: 505.5041. FT-IR (cm^{-1}, KBr): 3500–3096 (OH, broad), 3339 (NH), 1757 (s, C=O acid), 1646 (s, Amide I), 1559 (s, Amide II). UV–vis (CH_3OH, λ_{max} in nm, (ε) in cm^{-1}M^{-1}): 446 (250). ^{1}H NMR (δ in ppm, DMSO): 8.22 (2H, m, NH), 4.81 (1H, m, CH$^\alpha$-Asp merging with one of Cp H), 4.80 (4H, s, CH–Cp), 4.38 (4H, s, CH–Cp), 3.24 (2H, m, CH$_2^\beta$–Asp), 2.77 (2H, m, CH$_2^\beta$–Asp). ^{13}C{^{1}H} NMR (δ in ppm, DMSO-d$_6$): 171.1, 171.0 (C=O), 79.7 (C-substituted Cp), 72.3, 70.0 (C-unsubstituted Cp), 51.9, 51.1 (C–CH$^\alpha$ Asp), 35.6, 35.2 (C–CH$_2$ Asp).

2.4. Synthesis of 1,1′-Fc(CO–Glu–OEt)$_2$ (**4b-OEt**)

The reaction was analogous to that reported for **3b-OBz** using ferrocenedicarboxylic acid (0.85 g, 3 mM), HOBt (1.0 g, 6.6 mM), EDC (1.27 g, 6.6 mM),and H–Glu–(OEt)$_2$ · HCl (3 g). Column chromatography: hexane/EtOAc/CHCl$_3$ 4:3:3. R_f = 0.3. Yield: 0.53 g, 62.9%. HR-MS (FAB): calc. for C$_{30}$H$_{40}$N$_2$O$_{10}$Fe = 634.2032, found: 635.2927. FT-IR (cm^{-1}, KBr): 3475 (NH), 1747 (s, C=O ester), 1635 (s, Amide I), 1551 (s, Amide II). UV–vis (CH$_3$OH, λ_{max} in nm, (ε) in cm^{-1}M^{-1}): 440 (345). ^{1}H NMR (δ in ppm DMSO-d$_6$) 8.30 (2H, d, J = 8 Hz, NH–Glu), 4.35 (1H, m, CH$^\alpha$–Glu), 4.12 (2H, m, CH$_2$–O), 4.07 (2H, q, J = 7 Hz, CH$_2$–O), 4.88 (2H, s, CH–Cp), 4.82 (2H, s, CH–Cp), 4.42 (2H, s, CH–Cp),4.39 (2H, s, CH–Cp), 2.45 (2H, t, J = 7 Hz, CH$_2$–Glu), 2.09 (1H, m, CH$_2$–Glu), 1.96 (1H, m, CH$_2$–Glu), 1.21 (3H, t, J = 7 Hz, CH$_3$-ester), 1.17 (3H, t, J = 7 Hz, CH$_3$–ester). ^{13}C{^{1}H} NMR (δ in ppm DMSO-d$_6$) 173.1, 172.9, 170.0 (C=O), 77.5 (ipso C–Cp), 73.0, 72.8, 71.0, 70.3 (C, Cp), 52.3 (C$^\alpha$, Glu), 61.5, 60.8 (C–CH$_2$ ester), 31.0 (C–CH$_2$ Glu), 26.5 (C–CH$_2$ Glu), 14.9 (C–CH$_3$ ester).

2.5. Synthesis of 1,1′-Fc(CO–Glu–OH)$_2$ (**4b**)

The deprotection of the ester linkage was accomplished by base catalysed hydrolysis of **4b-OEt** (1.0 g, 1.5 mM) and 0.25 g of NaOH in wet MeOH. The reaction was complete after 30 min. After evaporation of the reaction mixture, the oily solid was purified by column chromatography using a solvent mixture of CHCl$_3$:MeOH:AcOH 17:2:1; R_f = 0.4. Yield: 0.44 g, 55%. HR-MS (FAB): calc. for C$_{22}$H$_{24}$N$_2$O$_{10}$Fe = 532.0780, found: 533.0548. FT-IR (cm^{-1}, KBr): 3500–3096 (w, br), 3350 (NH), 1754 (s, C=O ester), 1651 (s, Amide I), 1561 (s, Amide II). UV–vis (CH$_3$OH, λ_{max} in nm, (ε) in cm^{-1}M^{-1}): 446 (255). ^{1}H NMR (δ in ppm, DMSO-d$_6$): 7.87 (1H, d, NH), 4.86 (1H, m, CH$^\alpha$–Glu), 3.68 (1H, s, CH$^\alpha$–Glu), 4.95 (1H, d, H^o Cp), 4.77 (1H, s, H^o Cp), 4.43 (1H, s, H^m Cp), 4.36 (1H, s, H^m Cp), 3.58 (2H, m, CH$_2^\beta$-Glu), 2.40 (2H, m, CH$_2^\beta$-Glu), 2.02 (1H, m, CH$_2^\gamma$-Glu), 1.9 (1H, m, CH$_2^\gamma$-Glu). ^{13}C{^{1}H} NMR (δ in ppm, DMSO-d$_6$): 175.2, 173.7, 172.8, 169.8, 169.7 (C=O), 77.8, 77.7 (ipso C-substituted Cp), 72.7, 72.4, 70.7, 70.3 (C-unsubstituted Cp), 52.9, 52.2 (C–CH$^\alpha$ Glu), 31.7, 31.1, 26.9, 26.7 (C–CH$_2$ Glu).

2.6. Electrochemistry

All electrochemical experiments were carried out at room temperature (22 + 1 °C) on a CV-50W Voltammetric Analyzer (BAS) in aqueous buffered solutions using a three electrode cell system consisting of glassy carbon (BAS 3.0 mm diameter) as working electrode, Pt wire as counter electrode and Ag/AgCl (3.0 M KCl)

as the reference electrode; at scan rates of 100 mV/s). The carbon electrodes were cleaned by polishing on a micro-cloth pad with Al$_2$O$_3$ slurry (1.0 μm). The polished electrodes were rinsed with copious amount of water and tested in a background solutions before use. To ensure reproducibility the working electrode was cleaned between runs.

The determination of the acid–base properties of Fc-amino acids/peptides was studied by cyclic voltammetry on a 0.5 mM solution of the compound in 5% MeOH-aq. phosphate buffers between pH 2 and 8. Buffers were prepared with H$_3$PO$_4$, Na$_2$HPO$_4$, KH$_2$PO$_4$ to an ionic strength of 0.2 M. Where necessary, the pHs were adjusted by the addition of 1 M HCl or 1 M NaOH. pH measurements were carried out using an AccuMet (Fischer Scientific) combination glass electrode and standardized with VWR pH 4 and 7 buffer standards. The electrochemical response of the ferrocene–amino acid conjugates in the presence of either La^{3+}, Tb^{3+}, Zn^{2+}, Mg^{2+} or Ca^{2+} as guest cation species was investigated by CV and differential pulse voltammogram (DPV) by incremental aliquots of aqueous metal salts solutions to 5 ml, 0.5 mM solutions of the free acid in 0.1 M Tris–HCl buffer pH 6.8–7.0 and 0.2 M NaClO$_4$ supporting electrolyte. For the cyclic voltammetric (CV) studies the scan rates was 100 mV/s and for the DPV experiments a scan rate of 20 mV/s and pulse amplitude of 50 mV was used. Cyclic voltammograms (CVs) were scanned in the potential range of 0.4–1.1 V versus Ag/AgCl.

2.7. Synthesis of metal complexes of Fc–CO–Glu–OH

To a solution of metal triflates (20 mM) in 10 ml methanol:water (1:1), 10 ml of methanol/water (1:1) of Fc–CO–Glu–OH (10 mM) was added. The resulting pH of the solution was ca. 4. The pH was adjusted to 6.5 with dilute NaOH and stirred at room temperature for 12 h. Any precipitate formed was removed by filtration. The resulting orange suspension was concentrated to dryness and the residue picked up in 5 ml methanol and layered with diethylether to induce precipitation of the product. The solids were collected by filtration, washed with diethyl ether, and dried in vacuum. Complexes of the metals were analysed by ^{13}C NMR in DMSO-d$_6$ FT-IR as KBr pellets and electrospray ionization mass spectroscopy (ESI-MS). ESI-MS involved solutions prepared in 1:1 methanol/H$_2$O solution adjusted to pH 6.5 and analysed in positive ion mode.

3. Results and discussion

3.1. Synthesis and characterization

The 1,1′-disubstituted ferrocene–amino acids **2b–4b** were prepared by amidation of the acid group using

the carbodiimide method (EDC/HOBt) followed by basic ester hydrolysis (illustrated in Scheme 1). The related monosubstituted ferrocene–amino acids Fc–Gly–OH (**2a**), Fc–Asp–OH (**3a**) and Fc–Glu–OH (**4a**) were reported previously [34] (Scheme 2). All the compounds were characterized spectroscopically by ^{1}H and ^{13}C NMR, MS, UV–vis and FT-IR spectroscopy. Selected spectroscopic properties are summarized in Table 1.

The successful deprotection of the esters to the free acids is indicated by a lack of the resonances due to the protecting groups and the appearance of a resonance at δ 12.3–13.2 due to the acid OH. In addition, the IR shows a strong absorbance in the OH region. Fc-disubstituted compounds, **2b** and **3b**, show two typical singlets at δ 4.80 and δ 4.38, respectively, whereas four broad singlets were observed for **4b** at δ 4.90, 4.87, 4.42 and 4.37, similar to that observed for disubstituted ferrocene carbohydrate dendrimers [35].

The FT-IR spectra of the esters in solution and free acids in the solid state (KBr) reveal characteristic features of the ferrocene and the amino acid moieties (Table 1). Particularly, the position of the amide A band at 3400–3300 cm^{-1} is quite informative. Amide NH stretches below 3400 cm^{-1} are diagnostic of a compound that participates in hydrogen bonded (H-bonded) [36,37]. The amide A stretches of compounds **3a**, **4a** and **2b**–**4b** indicate H-bonded structures. H-bonding involving the two podant amino acid groups is a common structural motif in 1,1′-bis-amino acid substituted ferrocenes. In addition, the crystal structure of **2b** shows strong intramolecular H-bonding between the two amide groups on the two podant amino acid substitu-
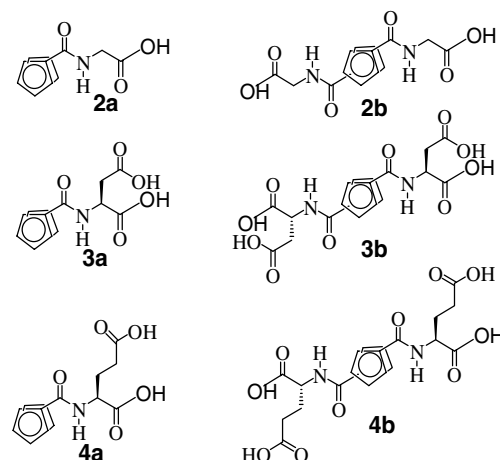
Scheme 2. Ferrocene–amino acid conjugates; Fc–Gly–OH **2a**, Fc–Asp–OH **3a**, Fc–GluOH acid **4a**; and 1,1′-disubstituted ferrocene–amino acid conjugates; Fc–(Gly–OH)$_2$ **2b**, Fc–(Asp–OH)$_2$ **3b**, Fc–(GluOH)$_2$ **4b**.

ents [34]. Thus, we suggest that **2b**, **3b**, and **4b** exist in the 1,2′-conformation, which supports intramolecular H-bonding between the two podant amino acids [38,39].

Circular dichroism (CD) spectra of the 1,1′-diacids and their esters in MeOH all showed an induced positive Cotton effect in the Ferrocene band at λ = 440 nm. which indicates a chirally organized structure assembled by intramolecular H-bonding (supporting information) [19].

3.2. Electrochemical studies

All Fc–amino acid conjugates **2a**–**4a** and **2b**–**4b** exhibit electrochemically and chemically fully reversible one-electron oxidation, as judged from the separation of the oxidative and reductive peak position and peak currents, respectively. These data are summarized in Table 2. The half wave potential ($E_{1/2}$) of some Fc conjugates was found to be sensitive to the pH of the solution (Supporting information Table S1 and Fig. S2) [40,41].

The interactions of Fc-amino acids with Mg^{2+}, Ca^{2+}, Zn^{2+}, La^{3+}, and Tb^{3+} were studied by CV and DPV. Fig. 1 shows a typical CV and DPV obtained for a solution of Fc–Asp–OH (**3a**) before and after the addition of 2 equivalents of a Tb^{3+} at pH 6.8, where the compound is fully deprotonated. Tables 3 and 4 summarize the electrochemical results. In all cases, addition of metal ions to the solution causes an anodic shift. For the mono-substituted acidic systems, Fc–Asp–OH (**3a**) and Fc–Glu–OH (**4a**), the addition of La^{3+} and Tb^{3+} caused large shifts in $E_{1/2}$ (Table 3) whereas, shifts caused by the addition of Mg^{2+} and Ca^{2+} were much smaller. Unexpectedly, addition of metal ions to the disubstituted Fc derivatives caused significantly smaller changes in $E_{1/2}$ for **3b** and **4b** whereas **2b** experienced a much greater shift, especially towards Mg^{2+} and Ca^{2+}. The anodic
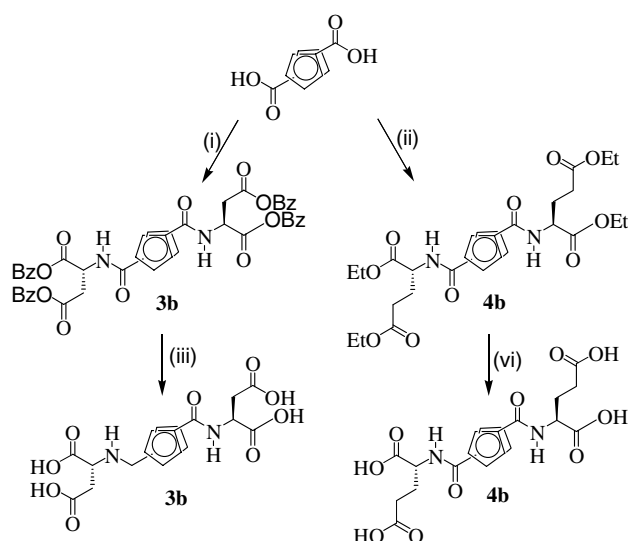
Scheme 1. Synthesis of 1,1′-disubstituted ferrocene–amino acid conjugates: (i) EDC, HOBt, H-Asp(OBz)$_2$ · Tos, Et$_3$N, CH$_2$Cl$_2$; (ii) H$_s$, Pd/C, MeOH (aq); (iii) EDC, HOBt, H–Glu(OEt)$_2$ · HCl, Et$_3$N; (iv) NaOH, MeOH.

Table 1
Selected spectroscopic parameters for Fc–amino acid conjugates

[1H] NMR[a] (ppm)						IR[b] (cm^{-1})			UV–vis[c] (nm(ε))
Compound	NH	H^o	H^m	Cp	COOH	NH	C=O ester/acid	C=O amide	
2a-OEt	8.31	4.80	4.39	4.24	–	3475	1747	1635	444 (260)
3a-OMe	8.23	4.80	4.37	4.20	–	3455	1739	1628	446 (220)
4a-OEt	8.01	4.89, 4.82	4.38	4.21	–	3434	1746	1640	442(240)
2a	8.14	4.79	4.35	4.24	12.77	3428	1756	1621	444 (210)
3a	7.98	4.80, 4.79	4.35	4.21	13.12	3344	1752	1600	442 (220)
4a	7.84	4.87, 4.82	4.36	4.21	12.40	3322	1733, 1717	1616	446 (255)
2b-OEt	8.30	4.85	4.44	–	–	3455	1740	1643	450 (320)
3b-OBz	8.30	4.80, 4.78	4.29	–	–	3446	1761	1646	449 (305)
4b-OEt	8.30	4.83, 4.82	4.42, 4.39	–	–	3475	1747	1635	440 (354)
2b	8.22	4.80	4.38	–	12.40	3385	1715	1593	460 (245)
3b	8.38, 8.01	4.83	4.38	–	12.38	3339	1757	1646	446 (250)
4b	8.12, 7.92	4.90, 4.87	4.42, 4.37	–	12.35	3350	1754	1651	446 (255)

[a] NMR at 1 mM concentration, in DMSO-d$_6$.
[b] IR were recorded in KBr for the monosubstituted compounds (**2–4a** and **2b-4b**) their esters spectra were recorded in CHCl$_3$ (6 mM).
[c] Recorded in MeOH solution at various concentrations (1–10 mM).

Table 2
Electrochemical data for Fc-modified compounds **2a–4a** and **2b–4b** from CV measurements

M^{n+}	2a	3a	4a
–	376 (69)	388 (76)	392 (87)
Mg^{2+}	424 (83)	394 (80)	400 (93)
Ca^{2+}	422 (80)	393 (88)	401 (130)
Zn^{2+}	412 (96)	403 (93)	421 (120)
La^{3+}	400 (90)	424 (110)	459 (120)
Tb^{3+}	398 (92)	452 (120)	471 (125)
	2b	**3b**	**4b**
–	632 (80)	636(83)	605 (80)
Mg^{2+}	744 (180)	646 (90)	611 (88)
Ca^{2+}	720 (144)	652 (81)	616 (80)
Zn^{2+}	646 (114)	652 (82)	625 (89)
La^{3+}	716 (180)	656 (83)	639 (82)
Tb^{3+}	669 (184)	678 (78)	655 (88)

$E_{1/2}$ values are reported in mV and numbers in parentheses are the peak separation ($\Delta E = E_{pc} - E_{pa}$) values in mV.
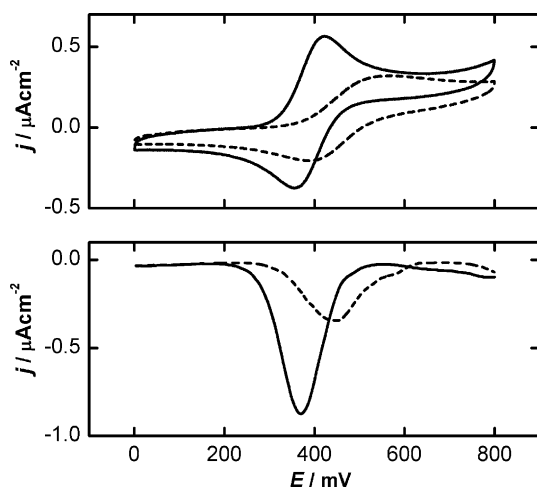

Fig. 1. CV and DPV plots for compound **3a** before (solid lines) and after(dashed line) addition of 2 equiv. of Tb^{3+} at pH 6.8.

shift is rationalized by a through space coulombic interaction of the metal centre and the positively charged ferrocenium [42,43]. Similarly, Beer and coworkers observed anodic shifts of 15, 35 and 55 mV for the interaction of a Fc–calixarene conjugate with La^{3+}, Gd^{3+} and Lu^{3+}, respectively. The interaction of the Fc-amino acids with La^{3+} and Tb^{3+}, experienced anodic shift that correlates with an increase of the ionic radii [9]. The change in $E_{1/2}$ between the free ligand and the complexed state ($\Delta E_{1/2}$), is indicative of the binding strength shown in the following equation [44]

$$\Delta E_{1/2} = E_{1/2}^{C} - E_{1/2}^{F} = \frac{RT}{nF} \cdot \ln\left(\frac{K_{red}}{K_{ox}}\right), \qquad (1)$$

where $E_{1/2}^{C}$, $E_{1/2}^{F}$ are the half-wave potentials for the complexed state and free ligand state, respectively; K_{red} and K_{ox} are the stability constants in the reduced and

Table 3
Electrochemical response of Fc-modified compounds to metal additions from CV measurements

	La^{3+} (1.06, 2.8)[a]		Tb^{3+} (0.92, 3.3)[a]		Mg^{2+} (0.86, 2.3)[a]		Ca^{2+} (0.99, 2.0)[a]		Zn^{2+} (0.74, 2.7)[a]	
	$\Delta E_{1/2}$	K_o/K_r	$\Delta E_{1/2}$	K_r/K_o	$\Delta E_{1/2}$	K_o/K_r	$\Delta E_{1/2}$	K_o/K_r	$\Delta E_{1/2}$	K_o/K_r
2a	24 (2)	2.5	22 (2)	2.3	48 (2)	6.3	46 (2)	5.9	36 (2)	4.0
3a	39 (2)	4.5	66 (2)	12.7	10 (4)	1.5	8 (4)	1.4	18 (4)	2.0
4a	57 (2)	13.7	80 (2)	21.7	12 (4)	1.6	16 (4)	1.9	29 (4)	3.1
2b	84 (2)	21.7	37 (2)	2.6	115 (4)	83.3	88 (4)	29.5	14 (4)	1.7
3b	20 (4)	2.2	42 (4)	5.0	11 (4)	1.5	16 (4)	2.5	13 (4)	1.6
4b	34 (4)	3.7	50 (4)	6.8	6 (4)	1.3	11 (4)	1.5	20 (4)	2.2

The values in parentheses represent the number of metal equivalents required to cause maximum change in $E_{1/2}$.
$\Delta E_{1/2} = E_{1/2}^{Complex} - E_{1/2}^{free}$.
[a] ionic radii of cation in Å and charge/size ratio.

Table 4
IR stretching frequencies (cm^{-1}) and ^{13}C NMR resonances (ppm) of selected peaks in M-2a and M-4a complexes

Assignment	2a	4a	2a-Mg^{3+}	2a-La^{3+}	4a-La^{3+}	4a-Mg^{2+}
v_{as}C=O			1556	1570	1550	1550
v_sC=O			1438(118)[a]	1445 (125)[a]	1440 (110)[a]	1445 (105)[a]
				1415 (155)[a]	1418 (132)[a]	
^{13}C=O (amide)	170.37	170.20	169.87 (0.50)[b]	169.67 (0.07)[b]	169.72 (0.48)	169.65 (0.55)[b]
^{13}C=O (acid)	172.42	174.80,	175.77 (3.35)[b]	174.97 (2.55)[b]	180.20 (5.70)	177.03 (2.23)[b]
		174.50			180.91 (6.11)	178.04 (3.54)[b]
^{13}CH$^\alpha$	41.64	52.09	43.69 (2.05)[b]	43.45 (1.81)[b]	54.54 (2.15)[b]	53.87 (1.79)[b]
^{13}CH$_2^\beta$	–	26.68	–	–	[c]	29.49(2.81)[b]
^{13}CH$_2^\gamma$	–	31.22	–	–	34.16(2.94)[b]	33.53 (2.31)[b]
Ipso ^{13}C(Cp)	76.77	76.64	77.53 (0.85)[b]	77.50 (0.73)[b]	77.51 (0.87)[b]	77.40 (0.76)[b]

[a] $[\Delta v] = v_{as}(C=O) - v_s(C=O)$.
[b] ^{13}C NMR shifts.
[c] Broadened peaks.

oxidized states, respectively and other symbols have their standard meanings. The use of DPV was particularly informative because it is a more sensitive technique than CV and shows the presence of minor peaks as seen in Fig. 1 at ca. 600 mV. The small peak at 600 mV was observed at higher concentration of lanthanides and is attributed to the formation oligomeric species in solution or the formation of insoluble hydroxide complexes (a common phenomenon at neutral pH's) [45]. The reduction in peak current after addition of the metal is due to changes in the diffusion coefficient of the complex compared to the free ligand caused by the increase in molecular weight as expected from the Randles–Sevcik equation.

The metal complexation results are summarized in Table 3. In general, binding to La^{3+} and Tb^{3+} is stronger for compounds 3a and 4a whereas, the Gly-substituted compounds, 2a and 2b, exhibit preference for Mg^{2+} over the other ions. Hall and Chu reported the results of a CV study investigating the co-ordination of alkaline earth and lanthanide metal cations to a series Fc-cryptants [3]. It was noted that there is a correlation between the $\Delta E_{1/2}$ and the charge:radius ratio of the metal ion. Similar trends were observed for surface immobilized

CV studies investigating glutathione complexes [46]. Thus, on the basis of charge:ionic size ratio (Tb^{3+} > La^{3+} > Zn^{2+} > Mg^{2+} > Ca^{2+}), we would expect lanthanides to show much larger shifts compared to the alkaline earth metals, as was observed for 3a and 4a. The preference of the Gly compounds, 2a and 2b, to bind with Mg^{2+} and Ca^{2+} is rationalized by its flexibility and its preference for smaller cations and lower coordination numbers. The stability constant for Gly–Mg^{2+}, –Ca^{2+} and –La^{3+} complexes were calculated as 3.44, 1.38 and 3.24, respectively, and the values for Asp for the same metals are 2.43, 1.60 and 3.42, respectively [47]. Therefore, it is not surprising to find that the Gly conjugates 2a and 2b show a higher affinity towards Mg^{2+} and Ca^{2+} compared to the Asp conjugates 3a, and 3b, and the Glu conjugates 4a and 4b.

The addition of the lanthanides to 4a resulted in a maximum anodic shift, $\Delta E_{1/2}$ after the addition of 2 mole equivalent of Ln^{3+} for the monosubstituted conjugates (see Fig. 2). The alkaline earth metals resulted in a negligible increase with metal additions. The disubstituted conjugates showed anodic shift maxima after 4 mol equiv. for all metals, except for lanthanides, which shows 2 mol equiv. for 2b (Table 3).
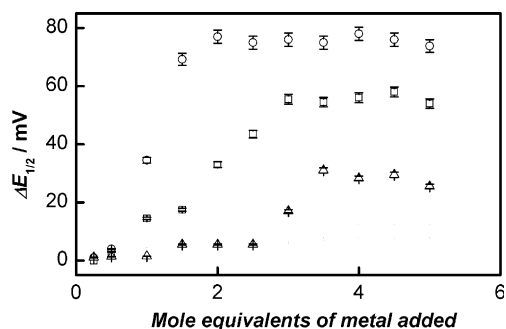
Fig. 2. Changes in $\Delta E_{1/2}$ with the addition of Tb^{3+} (○), La^{3+} (□) and Zn^{2+} (△) to **4a**. (Ca^{2+} and Mg^{2+} titrations were omitted because they showed negligible change in $\Delta E_{1/2}$).

3.3. Spectroscopic studies of metal complexation

Electrospray-ionization mass spectrometry (ESI-MS), IR and ^{13}C NMR spectroscopy were used to evaluate the structural properties of the metal complexes of the ferrocene–amino acid conjugates and the results are summarized in Table 4.

ESI-MS is a useful tool in the identification of metal complexes and allows deductions about the complexation behavior of ligands. The ESI-MS spectrum of a solution of ligand **4a** with Tb^{3+} is shown in Fig. 3. The spectrum shows peaks related to the ligand as well as the complex. The ligand is indicated by peaks m/z at 382.034 and 404.016 representing $[L + Na]^+$ and $[L − H + 2Na]^+$, respectively. The spectrum also shows a prominent peak at m/z 596.925, which is assigned to $[Tb_2L_2(H_2O)_9]^{2+}$ (L = **4a**) on the basis of modeling the correct isotopomer. The isotopic peaks are separated by 0.5 m/z units, which clearly reveals the +2 charge state of this ion. Other minor metal complex peaks such as $[M_2L_2(H_2O)_7(CH_3OH)]^{2+}$ are present at m/z 595.005, which shows the coordination of a solvent molecule and others peaks may represent more complex structures. A similar experiment for **2a** with Ca^{2+} and Tb^{3+}, showed
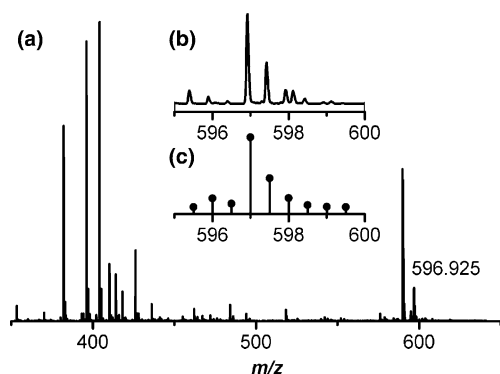

Fig. 3. (a) ESI-MS of $[M_2L_2(H_2O)_9]^{2+}$ of 4:1 (Tb^{3+}: **4a**) in 1:1 methanol/H_2O at pH 6.5. (b) Expanded region of the molecular ion. (c) The simulated isotopic ratio spectrum.

ligand peaks at m/z 287.023, 310.015 representing $[L + H]^+$ and $[L + Na]^+$, respectively and m/z 410.026, 559.994, are identified as $[ML(H_2O)_3(CH_3OH)]^+$ and $[ML(H_2O)_3(CH_3OH)]^+(CF_3SO_4)$ for the Ca^{2+} and 637.127, $[ML(H_2O)_9(CH_3OH)]^+$ of Tb^{3+} complexes, respectively.

The ^{13}C NMR clearly indicates the participation of the carboxylate group in the coordination to the metal centers. For complexes of **2a** and **4a** with metal ions, the carbon of the carboxylate group experienced downfield shifts of 3.0–6.0 ppm. The aliphatic C atoms of the side chain, including the α-C, experienced shifts that appear to be dependent on the distance from metal center. The shift generally decreased as the distance to the metal center increased ($\Delta\delta$ 2.8–3.5 ppm for the β-CH_2, $\Delta\delta$ 2.3–3.1 ppm for γ-CH_2, and $\Delta\delta$ 1.7–2.6 ppm for α-CH). The amide carbonyl and carbons of ferrocene showed shifts of less than 1.0 ppm indicating that they do not participate in binding of the metal ions. Such magnitudes of shifts have been reported for Asp and Glu, Phe and glutathione, with Pd^{2+} [48] and Ln^{3+} [5,8,49]. The downfield shifts of the carbonyl chemical shifts are consistent with complexation with the metals since it causes a decrease of the electron density around the corresponding carbon atom [49].

The difference between the symmetric and asymmetric stretching vibration of the carboxylate group (Δv) observed in the FT-IR spectra is a diagnostic tool that provides structural insight into the coordination mode of the carboxylate group [50,51]. Phillips recorded the frequencies of acetate ions in solutions containing alkaline metals, alkaline earth metals, and transitional metals and proposed an empirical relationship for Δv summarized as follows: ionic (164 cm^{-1}), bridging (140–170 cm^{-1}), bidentate (40–80 cm^{-1}), unidentate (200–300 cm^{-1}). Gericke and Huhnerfuss [52] also found empirical relationship from interactions of saturated fatty acids with metals; ionic (158 cm^{-1}), bridging bidentate (150–200 cm^{-1}) bidentate chelating (80–110 cm^{-1}). Our results suggests a bidentate chelating mode of coordination for alkaline earth metals with **2a** and **4a** (Δv between 110 and 105 cm^{-1}), and bidentate bridging and chelating modes for lanthanides complexes of **2a** and **4a** (Δv 135–155 cm^{-1} and 110–105 cm^{-1}, respectively). The amido and carboxylate functional groups bands of the metal complexes at 1550–1575 cm^{-1} in **2a** and **4a** are assigned to the antisymmetric stretching vibration $v_{as}(COO^-)$. The bands in the 1419–1435 cm^{-1} region are the symmetric stretching vibration $v_s(COO^-)$, consistent with established values of Mg^{2+}, Ca^{2+} and Ln^{3+} complexes of Glu, in which the v (COOH) was observed at 1700 cm^{-1}, $v_s(COO^-)$ at 1540–1680 cm^{-1}, and $v_{as}(COO^-)$ at 1410–1420 cm^{-1} [53–55]. After complexation, the characteristic C=O stretches in the free acid at 1756 and 1733, 1717 cm^{-1} for **2a** and **4a**, respectively, are absent, indicating metal

coordination. Furthermore, in the metal complexes the amide NH stretch is absent for ligand **2a**, suggesting either deprotonation or deprotonation and complexation. NH deprotonation was observed for Trp complexation of Eu^{3+} and is commonly observed in peptide complexes of Cu^{2+}, Ni^{2+} [56–59], and Co^{2+} [60–63].

Theoretical studies by Dudev and Lim [64] into the coordination behavior of carboxylates show that the charge density, the coordination number and other factors such as solvation are important. They contend that reducing the net charge on the metal ion disfavors the formation of a bidentate over a monodentate system. Furthermore, in water-rich octahedral Mg(II) complexes containing a single carboxylate, the bidentate structure is slightly more favored but monodentate is favored in cases where an additional binding ligand, especially water, which forms hydrogen bonded systems. Lastly, Dudev and Lim suggested that in complexes where two or more backbone ligands are available, the bidentate carboxylate mode is more stable than the corresponding monodentate mode. In the case of Ln^{3+}, where an increased coordination number is possible, the bidentate mode of coordination is favored. Our observations generally agree with reports by Torres and co-workers [65–71] who described extensively the coordination behavior of the carboxylate group with Ln^{3+}. Bidentate carboxylate coordination networks in the typical *syn–syn* bridging, chelate bidentate and tridentate modes have been observed before in the crystal structure of *N*-methylglycine Eu(III) complexes, glycine–Nd^{3+} complexes, as well as lanthanide glutamte and aspartate complexes [65–71].

4. Conclusions

In this study, we evaluated the interaction of the six Fc–amino acid conjugates Fc–CO–Gly–OH (**2a**), Fc–CO–Asp–OH (**3a**), Fc–CO–Glu–OH (**4a**), 1,1′-Fc(CO–Gly–OH) (**2b**), 1,1′-Fc(CO–Asp–OH) (**3b**), and 1,1′-Fc(CO–Glu–OH) (**4b**) with metal ions Mg^{2+}, Ca^{2+}, Zn^{2+}, La^{3+}, and Tb^{3+}. Using CV and DPV experiments, we showed that the Fc group is providing an electrochemical response to metal binding to the carboxylate. The Asp and Glu conjugates exhibit a small preference for the lanthanide ions and the Gly-substituted compounds **2a** and **2b** exhibit preference for Mg^{2+} and Ca^{2+}. Thus, we observe an interesting change in the selectivity for metal binding as a function of amino acid residue. The selectivity displayed by **3a** and **4a** towards binding of Ln^{3+} over alkaline earth metals can certainly be rationalized in terms of their charge to size ratio. Dudev and Lim's [64] theoretical study offer additional insight into the effect of carboxylate coordination on the type of metal, its coordination number, the total charge of the metal complex, immediate surroundings and rela-

tive solvent exposure of the metal binding site. Future experiments are aimed at exploring the coordination behavior of such amino acid and peptide conjugates which are covalently linked to a surface and monitor the influence of metal coordination on the electric properties of the interface.

Appendix A. Supplementary data

Supplementary data associated with this article can be found, in the online version at doi:10.1016/j.jorganchem.2004.11.027.

References

[1] H. Plenio, H. El-Desoky, J. Heinze, Chem. Ber. 126 (1993) 2403.
[2] H. Plenio, C. Aberle, Y.A. Shihadeh, J.M. Lloris, R. Martinez-Manez, T. Pardo, J. Soto, Chem. J. Eur. 7 (2001) 2848.
[3] C.D. Hall, S.Y.F. Chu, J. Organomet. Chem. 498 (1995) 221.
[4] Z. Chen, J.A. Pilgrim, P.D. Beer, J. Electroanal. Chem. 444 (1998) 209.
[5] B. Podanyi, R.S. Reid, J. Am. Chem. Soc. 110 (1988) 3805.
[6] J. Legendziewicz, H. Kozioski, B. Jezowska-Trzebiatowska, E. Huskowska, Inorg. Nuc. Lett. 15 (1979) 349.
[7] D.A. Sherry, C. Yoshida, E.R. Birnbaum, D.W. Darnall, J. Am. Chem. Soc. 95 (1973) 3011.
[8] J. Legendziewicz, E. Huskowska, H. Kozioski, B. Jezowska-Trzebiatowska, Inorg. Nuc. Lett. 17 (1981) 57.
[9] G.D. Brindley, O.D. Fox, P.D. Beer, J. Chem. Soc., Dalton Trans. (2000) 4354.
[10] H.G. Brittain, Inorg. Chem. 18 (1979) 1740.
[11] J.C. Pessoa, T. Gajda, R.D. Gillard, T. Kiss, S.M. Luz, J.J.G. Moura, I. Tomaz, J.P. Telo, I. Torok, J. Chem. Soc., Dalton Trans. (1998) 3587.
[12] P.D. Beer, Z. Chen, J. Pilgrim, J. Chem. Soc., Faraday Trans. (1995) 4331.
[13] E. Qutierrez, T.C. Miller, J.R. Gonzalez-Redondo, J.A. Holcombe, Environ. Sci. Technol. 33 (1999) 1664.
[14] D.C. Silverman, D.J. Kalota, F.S. Stover, Corros. Sci. 51 (1995) 818.
[15] W. Yang, J.J. Gooding, D.B. Hibbert, Analyst 126 (2001) 1573.
[16] W. Yang, E. Chow, G.D. Willett, D.B. Hibbert, J.J. Gooding, Analyst 128 (2003) 712.
[17] D. Freiesleben, K. Polborn, C. Robl, K. Sunkel, W. Beck, Can. J. Chem. 73 (1995) 1164.
[18] Z.H. Chohan, Metal Based Drugs 7 (2000) 177.

[19] T. Moriuchi, A. Nomoto, O. Yamauchi, A. Ogawa, T. Hirao, J. Am. Chem. Soc. 123 (2001) 68.

[20] S.K. Drake, K.L. Lee, J.J. Falke, Biochemistry 35 (1996) 6697.

[21] S.M. Gagne, M.X. Li, B.D. Sykes, Biochemistry 36 (1997) 4386.

[22] T. Ozawa, M. Fukuda, M. Nara, A. Nakamura, Y. Komine, K. Kohama, Y. Umezawa, Biochemistry 39 (2000) 14495.

[23] Y. Sharma, C.M. Rao, M.L. Narasu, S.C. Rao, T. Somasundaram, A. Gopalakrishna, D. Balasubramanian, J. Biol. Chem. 264 (1989) 12794.

[24] X. Chen, Y.-X. Zhou, Y.-M. Xu, Chin. Acta Biophys. Sinica 12 (1996) 389.

[25] J.L. Yang, H.J. Li, H.T. Yan, J. Chin. Rare Earth Soc. 10 (1992) 86.

[26] G.S. Lukat, A.M. Stock, J.B. Stock, Biochemistry 29 (1990) 5436.

[27] P. Ciancaglini, J.M. Pizauro, C. Curti, A.C. Tedesco, F.A. Leone, Int. J. Biochem. 22 (1990) 747.

[28] W. Bauer, K. Polborn, W. Beck, J. Organomet. Chem. 579 (1999) 269.

[29] K. Schlogel, Monatsh. Chem. 88 (1957) 601.

[30] H.-B. Kraatz, J. Lusztyk, G.D. Enright, Inorg. Chem. 36 (1997) 2400.

[31] M.V. Baker, H.-B. Kraatz, J.W. Quail, New J. Chem. 25 (2001) 427.

[32] H.-B. Kraatz, T.C. Sutherland, F.E. Appoh, Acta Cryst. E 59 (2003) m1174.

[33] G. Schachschneider, M. Wenzel, J. Labelled Compd. Radiopharm. 22 (1984) 235.

[34] F.E. Appoh, T.C. Sutherland, H.-B. Kraatz, J. Organomet. Chem. 689 (2004) 4669.

[35] P.R. Ashton, V. Balzani, M. Clemente-Leon, B. Colonna, A. Credi, N. Jayaraman, F.M. Raymo, J.F. Stoddart, M. Venturi, Chem. J. Eur. 8 (2002) 673.

[36] S.H. Gellman, G.P. Dado, G.-P. Liang, B.R. Adams, J. Am. Chem. Soc. 113 (1991) 1164.

[37] K.Y. Tsang, H. Diaz, N. Graciani, J.W. Kelly, J. Am. Chem. Soc. 116 (1994) 3988.

[38] D.R. van Staveren, T. Weyhermüller, N. Metzler-Noltre, J. Chem. Soc., Dalton Trans. (2003) 210.

[39] R.S. Herrick, R.M. Jarret, T.P. Curran, D.R. Dragoli, M.B. Flaherty, S.E. Lindyberg, R.A. Slate, L.C. Thornton, Tetrahedron Lett. 37 (1996) 5289.

[40] M. Chahma, J.S. Lee, H.-B. Kraatz, J. Organomet. Chem. 648 (2002) 81.

[41] A.N.J. Moore, D.D.M. Wayner, Can. J. Chem. 77 (1999) 681.

[42] J.H.R. Tucker, S.R. Collison, Chem. Soc. Rev. 31 (2002) 147.

[43] C. Caltagirone, A. Bencini, F. Demartin, F.A. Devillanova, A. Garau, F. Isaia, L.V.P. Mariani, U. Papke, L. Tei, V. Gaetano, Dalton Trans. (2003) 901.

[44] P.D. Beer, P.A. Gale, G.Z. Chen, J. Chem. Soc., Dalton Trans. (1999) 1897.

[45] R. Prados, L.G. Stadtherr, H.J. Donato, R.B. Martin, J. Inorg. Nucl. Chem. 36 (1974) 689.

[46] K. Takehara, M. Aihara, N. Ueda, Electroanalysis 6 (1994) 1083.

[47] M. Cefola, A.S. Tompa, A.V. Celiano, P.S. Gentile, Inorg. Chem. 1 (1962) 290.

[48] O. Yamauchi, A. Odani, J. Am. Chem. Soc. 103 (1981) 391.

[49] C.R. Carubelli, A.M.G. Massabni, S.R.d.A. Leite, J. Braz. Chem. Soc. 8 (1997) 597.

[50] G.B. Deacon, R.J. Phillips, Coord. Chem. Rev. 33 (1980) 227.

[51] J.E. Tackett, Appl. Spectrosc. 43 (1989) 483.

[52] A. Gericke, H. Huhnerfuss, Thin Solid Films 245 (1994) 74.

[53] I.V. Malorova, T.A. Formina, N.A. Dobrynima, Y.Y. Sevryugina, Khimiya 33 (1992) 565.

[54] M. Devereux, M. Jackman, M. McCann, M. Casey, Polyhedron 17 (1998) 153.

[55] H.-G. Yu, J.-X. Dong, Y. Liu, S.-S. Qu, J. Chem. Eng. Data 48 (2003) 1279.

[56] C.G. Agoston, K. Varnagy, A. Benyei, D. Sanna, G. Micera, I. Sovago, Polyhedron 19 (2000) 1849.

[57] W. Bal, M.I. Djuran, D.W. Margerum, E.T.G. Junior, M.A. Mazid, R.T. Tom, E. Nieboer, P.J. Sadler, J. Chem. Soc., Chem. Commun. (1994) 1889.

[58] H.C. Freeman, J.M. Guss, R.L. Sinclair, Acta Cryst. B 34 (1978) 2459.

[59] A.J. Stemmler, C.J. Burrows, J. Am. Chem. Soc. 121 (1999) 6956.

[60] W.S. Sheldrick, S. Hebb, J. Organomet. Chem. 377 (1989) 357.

[61] M.T. Barnet, H.C. Freeman, D.A. Buckingham, I.N. Hsu, D.v.d. Helm, J. Chem. Soc., Dalton Trans. (1970) 367.

[62] E.J. Evans, C.J. Hawkins, J. Rodgers, M.R. Snow, Inorg. Chem. 22 (1983) 34.

[63] R.D. Gillard, E.D. McKenzie, R. Mason, G.B. Robertson, Nature 209 (1966) 1347.

[64] T. Dudev, C. Lim, J. Phys. Chem. B 108 (2004) 4546.

[65] P.P. Gawryszewska, L. Jerzykiewicz, P. Sobota, J. Legandziewicz, J. Alloys Compd. 300–301 (2000) 275.

[66] R. Wang, H. Liu, M.D. Carducci, T. Jin, C. Zheng, Z. Zheng, Inorg. Chem. 40 (2001) 2743.

[67] T. Glowiak, N. Dao-Cong, J. Legendziewicz, Acta Cryst. C 42 (1986) 1491.

[68] I. Csoregh, E. Huskowska, J. Legendziewicz, Acta Cryst. C 48 (1992) 1030.

[69] J. Legendziewicz, E. Huskowska, A. Waskowska, G. Argay, Inorg. Chim. Acta 92 (1984) 151.

[70] J. Legendziewicz, E. Huskowska, G. Argay, A. Waskowska, J. Less-Common Met. 146 (1989) 33.

[71] B.Q. Ma, D.S. Zhang, S. Gao, T.Z. Jin, C.H. Yan, G.X. Xu, Angew. Chem. Int. Ed. 39 (2000) 3644.